RESEARCH PAPER

Green synthesis of palladium nanoparticles using broth of *Cinnamomum camphora* leaf

**Xin Yang · Qingbiao Li · Huixuan Wang · Jiale Huang · Liqin Lin ·
Wenta Wang · Daohua Sun · Yuanbo Su · James Berya Opiyo ·
Luwei Hong · Yuanpeng Wang · Ning He · Lishan Jia**

Abstract The development of dependable, environmentally benign processes for the synthesis of nanoscale materials is an important aspect of nanotechnology. In the present study, we report one-pot biogenic fabrication of palladium nanoparticles by a simple procedure using broth of *Cinnamomum camphora* leaf without extra surfactant, capping agent, and/or template. The mean size of palladium nanoparticles, ranging from 3.2 to 6.0 nm, could be facilely controlled by merely varying the initial concentration of the palladium ions. The polyols components and the heterocyclic components were believed to be responsible for the reduction of palladium ions and the stabilization of palladium nanoparticles, respectively.

Keywords Palladium · Nanoparticles ·
Synthesis · Green · Nanobiotechnology

X. Yang · Q. Li (✉) · H. Wang · J. Huang ·
L. Lin · W. Wang · D. Sun · Y. Su · J. B. Opiyo ·
L. Hong · Y. Wang · N. He · L. Jia
Department of Chemical and Biochemical Engineering,
College of Chemistry and Chemical Engineering, Xiamen
University, Xiamen 361005, People's Republic of China
e-mail: kelqb@xmu.edu.cn

X. Yang · Q. Li · H. Wang · J. Huang ·
L. Lin · W. Wang · Y. Su
National Engineering Laboratory for Green Chemical
Productions of Alcohols, Ethers and Esters, Key
Laboratory for Chemical Biology of Fujian Province,
Xiamen University, Xiamen 361005, People's
Republic of China

Introduction

Nanoscale materials have received considerable attention because their structure and properties differ significantly from those of atoms and molecules as well as those of bulk materials (Rosei 2004) The synthesis of nanomaterials with the desired quality is one of the most exciting aspects in modern nanoscience and nanotechnology (Bhattacharya and Gupta 2005). Moreover, ultrafine transition metal nanoparticles have attracted great interest due to their unique physical, chemical, and thermodynamic properties that have made them useful in such diverse fields as catalysis (Narayanan and El-Sayed 2005), electronics (Cui and Lieber 2001), optics (Eychmuller 2000), and even in biological and medical science (Salata 2004).

In the last decade, the utilization of biological systems has emerged as a novel and reliable method for the synthesis of nanoparticles due to a growing need to develop eco-friendly processes in nanomaterials syntheses (Bhattacharya and Gupta 2005; Mandal et al. 2006). A great deal of effort has been put into the biosynthesis of metal nanoparticles, using bacteria (Klaus et al. 1999; Fu et al. 2000; Nair and Pradeep 2002; Yong et al. 2002; Zhang et al. 2005; Fu et al. 2006), fungi (Mukherjee et al. 2001a, b; Ahmad et al. 2005), and plant (Gardea-Torresdey et al. 1999, 2002, 2003; Shankar et al. 2003a, b; Shankar et al. 2004a, b; Ankamwar et al. 2005; Chandran et al. 2006; Huang et al. 2007; Nadagouda and Varma 2008). From these studies, biosynthetic method employing live plant or

plant extract has emerged a simple and viable alternative to traditional chemical procedures and physical methods only in recent years. Gardea-Torresdey et al. (1999, 2002, 2003) firstly reported the preparation of gold and silver nanoparticles by living plants. Sastry et al. attained biosynthesis of metal nanoparticles by plant leaf extract (Shankar et al. 2003a, b; Shankar et al. 2004a, b; Ankamwar et al. 2005; Chandran et al. 2006). Our group demonstrated that sundried *Cinnamomum camphora* (*C. camphora*) leaf could be used to synthesize silver and gold nanoparticles in aqueous solutions at ambient conditions (Huang et al. 2007). The above synthetic techniques by plant extract or biomass exhibits the prospective application of plant bioresource for synthesis of metal nanoparticles.

Recently, the advances in fabrication of ultrafine palladium nanoparticles (PdNPs) have gained great importance due to their application both in heterogeneous and homogeneous catalysis, due to their high surface-to-volume ratio and their high surface energy (Narayanan and El-Sayed 2005). The usual synthetic methodologies for producing PdNPs involve chemical reduction of Pd(II) by alcohol (Teranishi and Miyake 1998), $NaBH_4$/ascorbic acid (Jana et al. 2000), N_2H_4 (Yonezawa et al. 2001), PEG (Luo et al. 2005), $CNCH_2COOK$ (Wang et al. 2004), or ascorbic acid (Sun et al. 2007), reduction of $Pd(OAc)_2$ by dimethylamine-borane in supercritical carbon dioxide (Kameo et al. 2003), thermally induced reduction of $Pd(Fod)_2$ in *o*-xylene (Ho and Chi 2004), and sonochemical reduction of $Pd(NO_3)_2$ (Nemamcha et al. 2006). Nevertheless, most of these processes were performed in the presence of various stabilizers to prevent the formation of undesired agglomerates or aggregates of PdNPs. Additionally, there are few reports concerning biological production of PdNPs by plant extract or biomass, where the biomass was usually found to act as both reducing agent and stabilizer. The only success was the recent demonstration by Nadagouda and Varma (2008), who showed production of PdNPs using coffee and tea extract. Unfortunately, they offered relatively scarce information regarding PdNPs.

In this study, broth of *C. camphora* leaf was first used to synthesize PdNPs at ambient conditions. Ultrafine PdNPs were obtained and their characteristics were examined by various techniques. It is important to point out that size control of PdNPs could be achieved by simply altering the initial concentration of Pd(II) ions. As is commonly known, *C. camphora* has been widely cultivated in South China. And it has been reported by our group that some antitumor components could be extracted from *C. camphora* leaf (Su et al. 2006). Therefore, we deem that some pharmaceutically valuable molecules could be retained after bioreduction and the as-prepared PdNPs might have potential application in nanomedicines. The approach appears to be a facile alternative to conventional methods of producing PdNPs.

Experimental

Materials

Palladium chloride ($PdCl_2$) was purchased from Sinopharm Chemical Reagent Co. Ltd, China and was used as received. *C. camphora* leaf used for the bioreduction was prepared using the same procedures as those in our previous study (Huang et al. 2007).

Synthesis of PdNPs

In order to obtain the broth of *C. camphora* leaf, the carefully weighted biomass, 4.0 g, was added to 200 ml deionized water in round-bottom flasks of 500 ml capacity. The mixtures were boiled for 5 min, and thereafter filtrated and the filtrate was used for further experiments. In a typical synthesis for PdNPs, an appropriate amount of concentrated aqueous $PdCl_2$ solution (0.226 mol L^{-1}) was added to 50 ml filtrate in conical flasks of 100 ml capacity at room temperature to obtain 1×10^{-3} mol L^{-1}, 3×10^{-3} mol L^{-1}, and 5×10^{-3} mol L^{-1} $PdCl_2$ solutions, respectively. The flasks were thereafter shaken at a rotation rate of 150 rpm in the dark at 30 °C.

Characterization of samples

UV–visible spectroscopy analysis was carried out on an UNICAM UV-300 spectrophotometer (Thermo Spectronic) over wavelengths from 250 to 800 nm at a resolution of 1 nm. Equivalent amounts of the suspension (0.5 ml) were diluted in a constant volume of deionized water (5 ml) and subsequently analyzed at room temperature. X-ray diffraction (XRD) measurement was performed on an X'Pert Pro X-ray Diffractometer (PANalytical BV, The Netherlands) operated at

a voltage of 40 kV and a current of 30 mA with Cu Kα radiation. After the reaction, the resulting solutions were centrifuged at a speed of 12,000 rpm for 10 min and the precipitates were dried at 60 °C overnight and collected for the determination of the formation of palladium.

Transmission electron microscopy (TEM) and high resolution transmission electron microscopy (HRTEM) images were obtained on a JEOL JEM-2100 Microscope at 200 keV. Samples for TEM were prepared by placing a drop of the suspension on carbon coated copper grids and allowing water to completely evaporate. Size distribution and average size of the nanoparticles were estimated on the basis of TEM micrographs with the assistance of Sigma-Scan Pro software (SPSS Inc, Version 4.01.003). Energy dispersive X-ray (EDX) and selected-area electron diffraction (SAED) analysis of PdNPs were performed on a Tecnai F30 Microscope.

X-ray photoelectron spectroscopy (XPS) analysis was performed on an American Perkin-Elmer PHI-1600 with a monochromatised microfocused Al X-ray source. The binding energy was calibrated by C1 s as reference energy (C1 s = 284.5 eV). The colloidal solution of PdNPs was centrifuged at a speed of 12,000 rpm for 10 min. After removal of the colorless supernatant, the precipitates were then redispersed in pure water to form a new suspension of PdNPs. Sample for XPS analysis was fabricated by dropping the suspension onto clean silicon and allowing water to completely evaporate.

The leaf biomass before bioreduction, the biomass residue after bioreduction and the resulting palladium nanoparticles were analyzed by Fourier transform infrared (FTIR) Nicolet Avatar 660 (Nicolet, USA). The leaf biomass before bioreduction was attained by completely drying of the leaf biomass at 60 °C. The biomass residue after bioreduction and the resulting palladium nanoparticles were obtained by centrifuging the resulting solution at 12,000 rpm for 10 min, and then the supernatant and the precipitates were completely dried at the same temperature, respectively.

Results and discussion

Formation of PdNPs by broth of *C. camphora* leaf

The formation of PdNPs was monitored by UV–visible spectroscopy in the 250–800 nm range. The
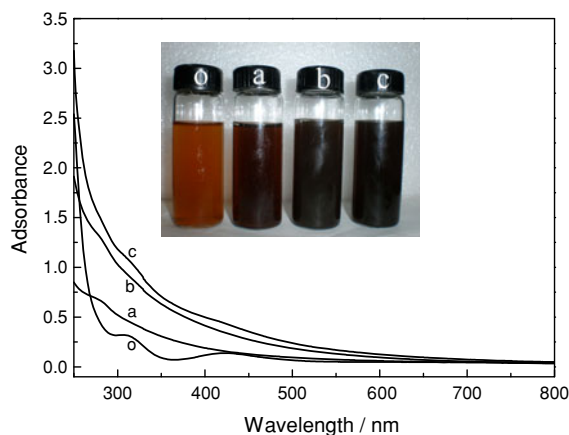
Fig. 1 UV–visible spectra of PdNPs prepared with different concentrations of $PdCl_2$ solution after bioreduction by *C. camphora* leaf broth at 30 °C for 48 h: (*a*) 1×10^{-3} mol L^{-1}; (*b*) 3×10^{-3} mol L^{-1}; (*c*) 5×10^{-3} mol L^{-1} and (*o*) UV–visible spectrum of 1×10^{-3} mol L^{-1} $PdCl_2$ solution. The inset shows a digital image of the as-prepared palladium colloidal solution and the $PdCl_2$ solution before reaction

color of the solution gradually turned from brownish-yellow into dark brown in 12 h, indicating the generation of PdNPs. Figure 1 displays the absorption spectra of palladium colloidal suspensions after 48 h of bioreduction by *C. camphora* leaf broth and the absorption spectra of $PdCl_2$ solution, used for comparison. The absorption bands appearing in the contrast spectrum of $PdCl_2$ solution were ascribed to the ligand-to-metal charge-transfer transition of the Pd(II) ions (Yonezawa et al. 2001; Luo et al. 2005; Ho and Chi 2004; Nemamcha et al. 2006). The absence of the absorption peaks above 300 nm in all the samples revealed the complete reduction of the initial Pd(II) ions (Yonezawa et al. 2001; Luo et al. 2005). The same accreditation was made by Ho and Chi (2004) and Nemamcha et al. (2006) during thermally induced reduction of Pd(Fod)$_2$ in *o*-xylene and sonochemical reduction of Pd(NO$_3$)$_2$ in aqueous solution, respectively. Moreover, Ho and Chi (2004) pointed out that the absence of these absorption peaks was consistent with the theoretical study of the surface plasmon resonance absorption of PdNPs. The spectra of the palladium colloidal suspensions presented broad absorption continua extending throughout the visible-near-ultraviolet region, which were typical of those of PdNPs (Teranishi and Miyake 1998; Yonezawa et al. 2001; Luo et al. 2005; Ho and Chi 2004; Nemamcha et al. 2006). This suggested the

formation of palladium colloid having a particle size of less than 10 nm, as described by Nemamcha et al. (2006).

Characterization of PdNPs

The morphology and size of PdNPs in the colloidal solutions and their size distribution were investigated by TEM. Figure 2 displays the TEM images of typical nanoparticles synthesized with *C. camphora* leaf and PdCl$_2$ solution of different concentrations at various magnifications. The initial concentration of the Pd(II) was found to have a vital impact on size and size distribution of PdNPs. For sample A (1×10^{-3} mol L^{-1}), the resulting PdNPs were well dispersed but quantitatively sparse (Fig. 2a–c). It might result from the relative insufficiency of the palladium precursor. In addition, some particles with irregular contour could be observed probably due to the effect of Ostwald ripening. According to size distribution of the PdNPs shown in Fig. 3a, the nanoparticles, mostly ranging from 3.6 to 9.9 nm in size, have a mean diameter of 6.0 nm. However, a further increase of initial Pd(II) concentration led to the formation of quasi-spherical nanoparticles with a narrower size distribution (Fig. 3b, c). Interestingly, the inter-particle distance of PdNPs was more uniformly dispersed and well aligned (Fig. 2d–i). The nanoparticles mainly range from 3.0 to 5.0 nm and from 2.2 to 4.3 nm in size, with mean particle diameters of 4.0 nm and 3.2 nm for samples B (3×10^{-3} mol L^{-1}) and C (5×10^{-3} mol L^{-1}), respectively. Apparently, it was found that the higher the concentration of the PdCl$_2$ solution, the smaller the PdNPs formed.

The particles were verified to contain a great deal of palladium according to EDX analysis in Fig. 4. The crystalline phase of the synthesized nanoparticles was confirmed by XRD (Fig. 5) and HRTEM (Fig. 6a). From the XRD patterns, prominent Bragg reflections at 2θ values of 40.0, 46.1, 67.9, 82.0, and 86.0 were observed, which correspond to the {111}, {200}, {220}, {311}, and {222} Bragg reflections of face-centered cubic (fcc) PdNPs. All the palladium nanoparticles in the HRTEM image showed lattice images, indicating that they are single crystallites. Figure 6b shows the SAED pattern recorded from the corresponding PdNPs. The ring-like diffraction pattern could be indexed on the basis of the fcc structure of palladium. Ring 1, 2, 3 arise due to reflections from {111}, {200}, {220} lattice planes of fcc palladium, respectively. HRTEM images, XRD patterns, and the SAED pattern thus clearly show that the PdNPs are crystalline in nature.

An XPS spectrum of the Pd 3d region (Pd 3d5/2 and Pd 3d3/2) for the obtained nanoparticles is shown in Fig. 7. The binding energy values are 335.4 ev for Pd 3d5/2 and 340.6 ev for Pd 3d3/2. The observed binding energy values for Pd 3d coincide with the reported data of Pd(0) within the experimental errors (Moulder et al. 1992). Quantitavive surface comoposition of the PdNPs determined by XPS is represented by C (45.8 atom%), O(33.7 atom%), Si (16.2 atom%), N (2.0 atom%), Pd (1.7 atom%), and Cl (0.6 atom%). Thereamong the three elements (C, O, N) originate from the biomass residue of *C. camphora* leaf broth. The trace amounts of Cl, which was not fully removed, may originate from the metal precursor.

Formation mechanism of PdNPs

Representative FTIR spectra of *C. camphora* leaf broth before and after the reaction are presented in Fig. 8. Some pronounced absorbance bands centered at 1037 cm^{-1}, 1079 cm^{-1}, 1122 cm^{-1}, 1226 cm^{-1}, 1267 cm^{-1}, 1322 cm^{-1}, 1384 cm^{-1}, 1459 cm^{-1}, 1515 cm^{-1}, 1631 cm^{-1}, 1730 cm^{-1} are observed in the region 1,000–1,800 cm^{-1}. Therein the absorbance bands at 1037 cm^{-1}, 1079 cm^{-1}, and 1122 cm^{-1} in Curve 1 could be assigned to the stretch vibration of –C–O (Stuart 2004). The sharpest band at 1,631 cm^{-1} might result from conjugated –C=C (Stuart 2004). The absorbance band at 1,730 cm^{-1} in Curve 2 could be assigned to the stretch vibration of -C=O (Stuart 2004). The comparison provided information concerning the chemical transformation of the functional groups involved in reduction of palladium ions. In the first place, it is clear that the absorbance bands at 1037 cm^{-1}, 1079 cm^{-1}, and 1122 cm^{-1} were weakened after the reaction. These bands might be assigned to the stretch vibration of –C–O (Stuart 2004). Previously, our group demonstrated that various components such as alkaloids, flavones, hydroxybenzenes, anthracenes, steroids, terpenoids, coumarins, lactones, linalools, polysaccharides, amino acids, and proteins existed in *C. camphora* leaf (Su et al. 2006). Thereby, we could infer that the polyols such as flavones, terpenoids, and polysaccharides in the broth played a critical role in reduction of Pd(II) ions. In the
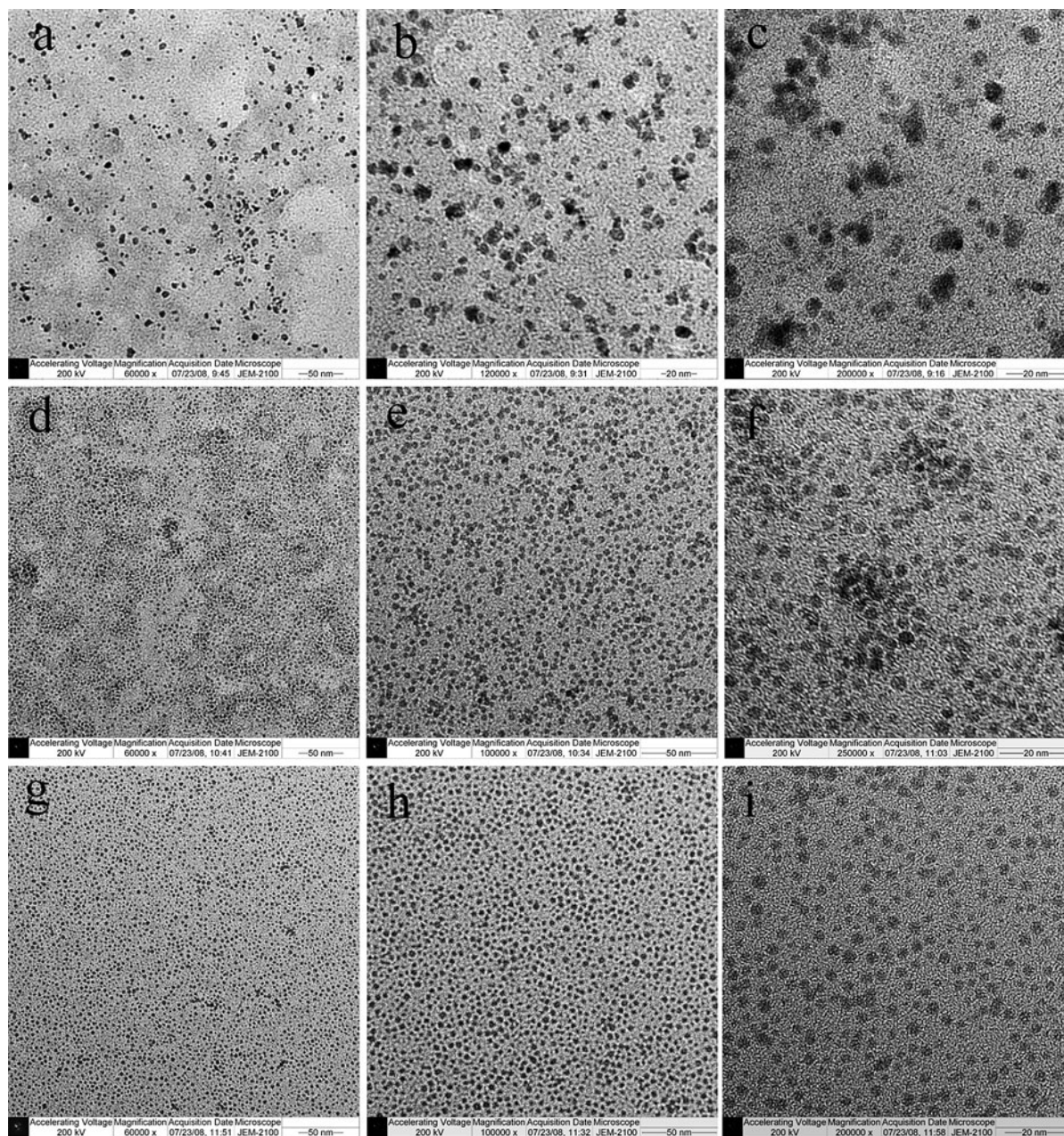
Fig. 2 TEM images of PdNPs after bioreduction. 50 ml leaf broth reacted with **a–c** 1×10^{-3} mol L^{-1}, **d–f** 3×10^{-3} mol L^{-1} and **g–i** 5×10^{-3} mol L^{-1} $PdCl_2$ at 30 °C, respectively

next place, the freshly appeared band at 1,730 cm^{-1} in Curve 2 could be ascribed to the stretch vibration of carbonyl groups. Hence, it is speculated that the polyols are oxidized to aldehydes or ketones and induce the formation of the band 1,730 cm^{-1}. In our previous study, the disappearance of the band at

1,109 cm^{-1} after bioreduction implied that the polyols from the sundried *C. camphora* leaf were mainly responsible for the reduction of silver ions or chloroaurate ions (Huang et al. 2007). Owing to this result and considering the application of as-prepared PdNPs in catalysis, the water-soluble components were
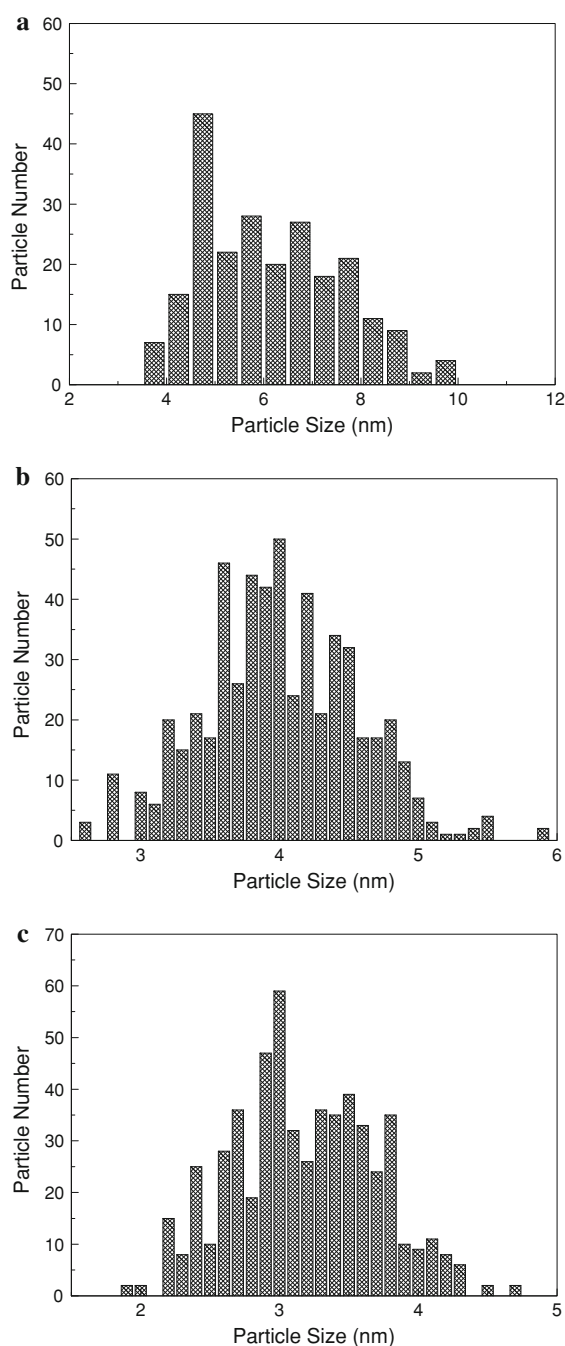
Fig. 3 A histogram of size distribution of PdNPs synthesized by reacting 50 ml leaf broth with 1×10^{-3} mol L^{-1} **a**, 3×10^{-3} mol L^{-1} **b**, and 5×10^{-3} mol L^{-1} **c**, PdCl$_2$ at 30 °C

extracted from the leaf and used in this study. Here, it is further confirmed that the water-soluble fractions in the leaf broth played a leading role in bioreduction of the precursors.

A typical FTIR spectrum of the obtained PdNPs is shown in Fig. 9, where the spectrum of *C. camphora* leaf broth before the reaction is also displayed for comparison. Several absorption peaks located at about 1384 cm^{-1}, 1461 cm^{-1}, 1515 cm^{-1}, and 1635 cm^{-1}, were observed in the region 1,000–1,800 cm^{-1}. Among them, absorption peaks at about 1384 cm^{-1}, 1461 cm^{-1}, 1515 cm^{-1}, and 1635 cm^{-1} remained nearly the same, while a new absorption peak emerged at 1,723 cm^{-1}. The wide absorption spectra at about 1,635 cm^{-1} might result from the stretch vibration of –C=C (Stuart 2004). And the absorbance band at 1,723 cm^{-1} could be ascribed to the stretch vibration of -C=O (Stuart 2004). In order to a great extent, the functional groups such as –C=C and –C=O, might derive from the water-soluble heterocyclic compounds in the *C. camphora* leaf broth. From the XPS analysis, one can also deduce that large amounts of C and O elements existed as part of the surface composition of the PdNPs, where the elements of C and O are very likely to bind to the surface of the PdNPs via some functional groups such as –C=C and –C=O. Consequently, it is deemed that the water-soluble heterocyclic compounds, e.g., alkaloids, flavones, acted as the stabilizer of the PdNPs. In the chemical routes to PdNPs, PVP is often used as capping ligands of the nanoparticles, where it is certain that the stabilization of PdNPs results from the adsorption of the PVP chain onto the particle surface via the coordination of the PVP –C=O group to the palladium atoms (Teranishi and Miyake 1998; Nemamcha et al. 2006). Similarly, the water-soluble heterocyclic compounds in the *C. camphora* leaf broth could specifically adsorb onto the particle surface via –C=O or –C=C to protect the PdNPs.

On the basis of the results of the above FTIR spectra and the fore-mentioned techniques such as XRD, HRTEM, SAED, and XPS, it is believed that a redox reaction took place between the hydroxyl group of the polyols in the *C. camphora* leaf broth and the Pd(II) ions. Ho Kim and Nakano (2005), who demonstrated adsorption of palladium by redox within condensed-tannin gel, proposed a redox reaction pathway between hydroxyl group of natural condensed-tannin gel and the Pd(II) species. Likewise, the reaction between broth of *C. camphora* leaf and the Pd(II) species might occur according to the following equation:

Fig. 4 EDX spectrum of PdNPs resulted from the fore-mentioned experiment using 5×10^{-3} mol L^{-1} solution of $PdCl_2$
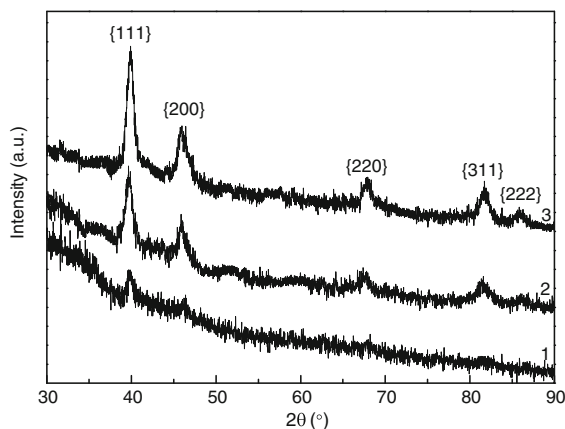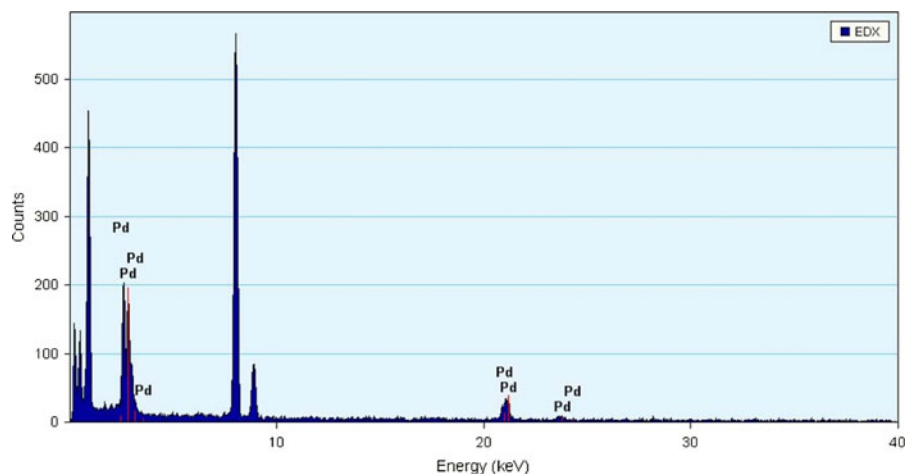

Fig. 5 XRD patterns of the as-prepared PdNPs. Labeled peaks correspond to the characteristic diffraction peaks of elemental Pd(0). Pattern 1, 2, and 3 were derived from XRD analysis of the dried palladium sol after reaction of 50 ml leaf broth with 1×10^{-3} mol L^{-1}, 3×10^{-3} mol L^{-1}, and 5×10^{-3} mol L^{-1} solution of $PdCl_2$, respectively

$$nPd(II) + 2R-(OH)_n \rightarrow nPd(0) + 2nR=O + 2nH^+ \quad (1)$$
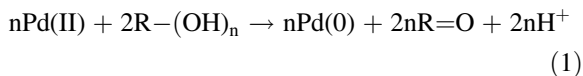
where R and n represent heterocycle or alkyl groups and the number of the hydroxyl groups oxidized by Pd(II) species, respectively. Hereby, it is reasonable to speculate that polyol components in the *C. camphora* leaf were oxidized into aldehydes or ketones while Pd(II) was reduced to elemental palladium. And the small decrease of pH of the resulting solution further confirmed the production of H^+ ions. The pH of the solution before the reaction was 2.00, 1.65, 1.54 for Samples A, B, and C, respectively, whereas

the pH of the solution after 48 h reaction became 1.86, 1.51, and 1.45 for Samples A, B, and C, respectively.

From the TEM results, one may conclude that the higher the concentration of the $PdCl_2$ solution, the smaller the PdNPs. On the contrary, Ho et al. (2005) stated that the higher the concentrations of the precursor, the larger the PdNPs during thermally induced reduction of Pd(Fod)$_2$ in *o*-xylene. This was truly interesting since our synthetic experiment was repeated twice and the same results were attained. The causation of such phenomena might be speculated as follows. In general, a higher concentration of the precursor would lead to a greater rate of generation of palladium atoms (Cushing et al. 2004). For sample B and C, it is very likely that a higher concentration of Pd(II) ions resulted in the full reduction of the initial Pd(II) ions at the commencement of the reaction. Although the nucleation process was relatively fast, the growth process remained comparatively slow due to the protective effects of sufficient biomolecules. This would diminish the effect of Ostwald ripening (Cushing et al. 2004). Hence, smaller PdNPs that were uniformly separated and well aligned were obtained. In contrast, for the lowest initial Pd(II) concentration (sample A), it was observed that the PdNPs became larger in size and the width of the size distribution was fairly broad as can be seen in Fig. 2a–c. It was probably attributed to the Ostwald ripening process as well as the presence of unreduced palladium ions and partly reduced palladium atoms (Narayanan and El-Sayed 2005). Because of comparatively smaller reductive rate of
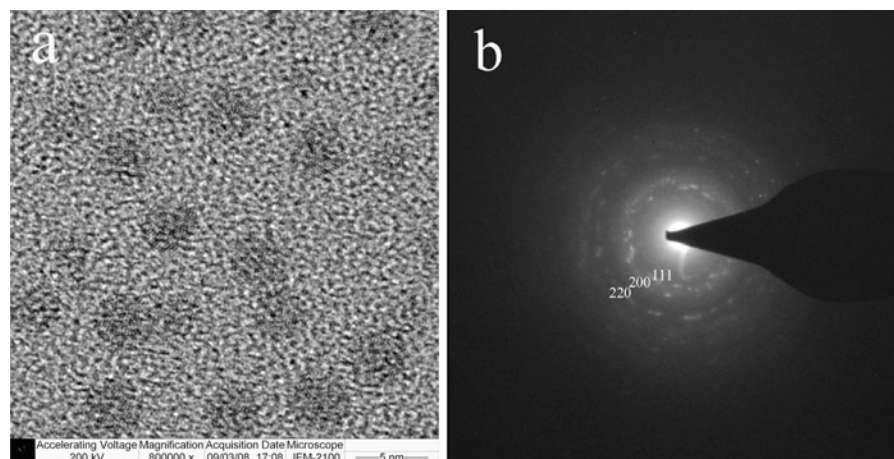
Fig. 6 HRTEM image (**a**) and SAED pattern (**b**) of PdNPs synthesized by reacting 50 ml leaf broth with 5×10^{-3} mol L^{-1} solution of $PdCl_2$
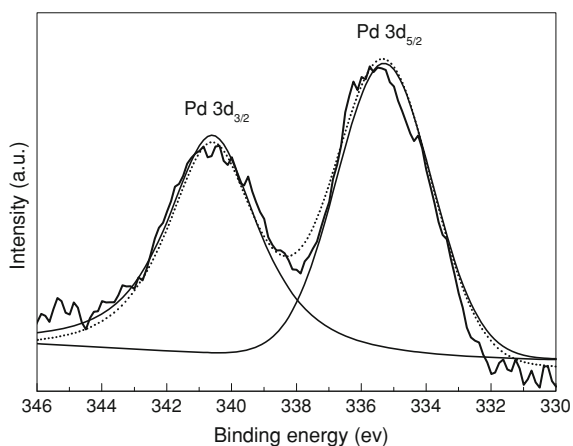
Fig. 7 XPS spectra of the Pd 3d region of the obtained nanoparticles
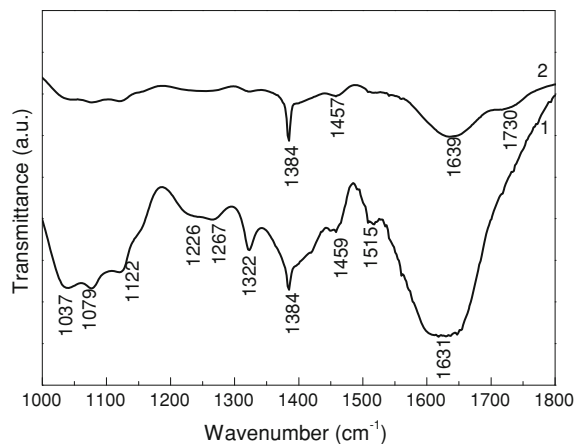
Fig. 8 Typical FTIR spectra of the leaf biomass before bioreduction (*1*), after bioreduction of palladium ions (*2*)

palladium ions, the palladium atoms freshly produced were inclined to attach to the more stable surfaces of the larger nanoparticles while there was detachment of surface atoms from the smaller nanoparticles to some extent (Narayanan and El-Sayed 2005). That is to say Ostwald ripening might be promoted and become significant in this situation. As a consequence, they tended to consume some smaller particles to form larger particles, and thus resulted in the formation of some irregular PdNPs with much broader size distribution. Although additional efforts are needed to investigate the detailed mechanism underlying the process of the reaction, this biological

synthetic technique offers an exciting new tool for the synthesis of PdNPs.

Conclusions

In conclusion, we developed a simple biological procedure to synthesize PdNPs using broth of *C. camphora* leaf. The size of PdNPs could be easily controlled by variation of the initial concentration of Pd(II) ions. XPS results confirmed the formation of metallic PdNPs. HRTEM images, XRD patterns, and the SAED pattern suggested the PdNPs were
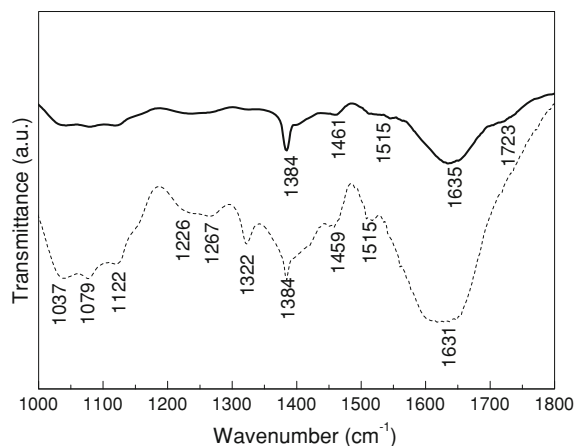
Fig. 9 Typical FTIR spectrum of the dried PdNPs (*the solid line*). The dash line shows the spectrum of the leaf biomass before bioreduction

essentially crystalline and characteristic of an fcc structure. The polyols components and the heterocyclic components were deemed to be responsible for the reduction of palladium ions and the stabilization of PdNPs, respectively. From a technological point of view, these obtained PdNPs may have potential applications not only in catalysis, but also in the medical field.

References

Ahmad A, Senapati S, Khan MI, Kumar R, Sastry M (2005) Extra-/intracellular biosynthesis of gold nanoparticles by an alkalotolerant fungus, *Trichothecium* sp. J Biomed Nanotechnol 1:47–53

Ankamwar B, Chaudhary M, Sastry M (2005) Gold nanotriangles biologically synthesized using tamarind leaf extract and potential application in vapor sensing. Synth React Inorg Met-Org Nano-Metal Chem 35:19–26

Bhattacharya D, Gupta RK (2005) Nanotechnology and potential of microorganisms. Crit Rev Biotechnol 25:199–204

Chandran SP, Chaudhary M, Pasricha R, Ahmad A, Sastry M (2006) Synthesis of gold nanotriangles and silver nanoparticles using aloe vera plant extract. Biotechnol Prog 22:577–583

Cui Y, Lieber CM (2001) Functional nanoscale electronic devices assembled using silicon nanowire building blocks. Science 291:851–853

Cushing BL, Kolesnichenko VL, O'Connor CJ (2004) Recent advances in the liquid-phase syntheses of inorganic nanoparticles. Chem Rev 104:3893–3946

Eychmuller A (2000) Structure and photophysics of semiconductor nanocrystals. J Phys Chem B 104:6514–6528

Fu J, Liu Y, Gu P, Tang D, Lin Z, Yao B, Wen S (2000) Spectroscopic characterization on the biosorption and bioreduction of Ag(I) by *lactobacillus* sp. A09. Acta Phys-chim Sin 16:779–782

Fu M, Li Q, Sun D, Lu Y, He N, Deng X, Wang H, Huang J (2006) Rapid preparation process of silver nanoparticles by bioreduction and their characterizations. Chin J Chem Eng 14:114–117

Gardea-Torresdey JL, Tiemann KJ, Gomez E, Dokken K, Tehuacanero S, Jose-Yacaman M (1999) Gold nanoparticles obtained by bio-precipitation from gold(III) solutions. J Nanopart Res 1:397–404

Gardea-Torresdey JL, Parsons JG, Gomez E, Peralta-Videa J, Troiani HE, Santiago P, Jose-Yacaman M (2002) Formation and growth of Au nanoparticles inside live alfalfa plants. Nano Lett 2:397–401

Gardea-Torresdey JL, Gomez E, Peralta-Videa J, Parsons JG, Troiani H, Jose-Yacaman M (2003) Alfalfa Sprouts: a natural source for the synthesis of silver nanoparticles. Langmuir 19:1357–1361

Ho Kim Y, Nakano Y (2005) Adsorption mechanism of palladium by redox within condensed-tannin gel. Water Res 39:1324–1330

Ho PF, Chi KM (2004) Size-controlled synthesis of Pd nanoparticles from β-diketonato complexes of palladium. Nanotechnology 15:1059–1064

Huang J, Li Q, Sun D, Lu Y, Su Y, Yang X, Wang H, Wang Y, Shao W, He N, Hong J, Chen C (2007) Biosynthesis of silver and gold nanoparticles by novel sundried *Cinnamomum camphora* leaf. Nanotechnology 18:105104

Jana NR, Wang ZL, Pal T (2000) Redox catalytic properties of palladium nanoparticles: surfactant and electron donor-acceptor effects. Langmuir 16:2457–2463

Kameo A, Yoshimura T, Esumi K (2003) Preparation of noble metal nanoparticles in supercritical carbon dioxide. Colloids Surf A 215:181–189

Klaus T, Joerger R, Olsson E, Granqvist C (1999) Silver-based crystalline nanoparticles, microbially fabricated. Proc Natl Acad Sci 96:13611–13614

Luo C, Zhang Y, Wang Y (2005) Palladium nanoparticles in poly(ethyleneglycol): the efficient and recyclable catalyst for Heck reaction. J Mol Catal A 229:7–12

Mandal D, Bolander ME, Mukhopadhyay D, Sarkar G, Mukherjee P (2006) The use of microorganisms for the formation of metal nanoparticles and their application. Appl Microbiol Biotechnol 69:485–492

Moulder JF, Stickle WF, Sobol PE, Bomben K (1992) Handbook of X-ray photoelectron spectroscopy. Perkin-Elmer Corporation, Eden Prairie

Mukherjee P, Ahmad A, Mandal D, Senapati S, Sainkar SR, Khan MI, Ramani R, Parischa R, Kumar PAV, Alam M, Sastry M, Kumar R (2001a) Bioreduction of AuCl$_4^-$ ions by the fungus, *Verticillium* sp and surface trapping of the

gold nanoparticles formed. Angew Chem Int Ed 40:3585–3588

Mukherjee P, Ahmad A, Mandal D, Senapati S, Sainkar SR, Khan MI, Parischa R, Ajaykumar PV, Alam M, Kumar R, Sastry M (2001b) Fungus-mediated synthesis of silver nanoparticles and their immobilization in the mycelial matrix: a novel biological approach to nanoparticle synthesis. Nano Lett 1:515–519

Nadagouda MN, Varma RS (2008) Green synthesis of silver and palladium nanoparticles at room temperature using coffee and tea extract. Green Chem 10:859–862

Nair B, Pradeep T (2002) Coalescence of nanoclusters and formation of submicron crystallites assisted by *Lactobacillus* strains. Cryst Growth Des 2:293–298

Narayanan R, El-Sayed MA (2005) Catalysis with transition metal nanoparticles in colloidal solution: nanoparticle shape dependence and stability. J Phys Chem B 109:12663–12676

Nemamcha A, Rehspringer J, Khatmi D (2006) Synthesis of palladium nanoparticles by sonochemical reduction of palladium(II) nitrate in aqueous solution. J Phys Chem B 110:383–387

Rosei F (2004) Nanostructured surfaces: challenges and frontiers in nanotechnology. J Phys Condens Matter 16:S1373–S1436

Salata OV (2004) Applications of nanoparticles in biology and medicine. J Nanobiotechnol 2:3

Shankar SS, Ahmad A, Pasricha R, Sastry M (2003a) Bioreduction of chloroaurate ions by geranium leaves and its endophytic fungus yields gold nanoparticles of different shapes. J Mater Chem 13:1822–1826

Shankar SS, Ahmad A, Sastry M (2003b) Geranium leaf assisted biosynthesis of silver nanoparticles. Biotechnol Prog 19:1627–1631

Shankar SS, Rai A, Ahmad A, Sastry M (2004a) Rapid synthesis of Au, Ag, and bimetallic Au core—Ag shell nanoparticles using neem (Azadirachta indica) leaf broth. J Colloid Interface Sci 275:496–502

Shankar SS, Rai A, Ankamwar B, Singh A, Ahmad A, Sastry M (2004b) Biological synthesis of triangular gold nanoprisms. Nat Mater 3:482–488

Stuart B (2004) Infrared spectroscopy: fundamentals and applications. Wiley-VCH Verlag Gmbh & Co. KGaA, Weinheim

Su Y, Li Q, Yao C, Lu Y, Hong J (2006) Antitumor action of ethanolic extractives from camphor leaves. Chin Chem Ind Eng Prog 25:200–204

Sun Y, Zhang L, Zhou H, Zhu Y, Sutter E, Ji Y, Rafailovich MH, Sokolov JC (2007) Seedless and templateless synthesis of rectangular palladium nanoparticles. Chem Mater 19:2065–2070

Teranishi T, Miyake M (1998) Size control of palladium nanoparticles and their crystal structures. Chem Mater 10:594–600

Wang Z, Shen B, He N (2004) The synthesis of Pd nanoparticles by combination of the stabilizer of $CNCH_2COOK$ with its reduction. Mater Lett 58:3652–3655

Yonezawa T, Imamura K, Kimizuka N (2001) Direct preparation and size control of palladium nanoparticle hydrosols by water-soluble isocyanide ligands. Langmuir 17:4701–4703

Yong P, Rowson N, Farr JPG, Harris I, Macaskie L (2002) Bioreduction, biocrystallization of palladium by Desulfovibrio desulfuricans NCIMB 8307. Biotechnol Bioeng 80:369–379

Zhang H, Li Q, Lu Y, Sun D, Lin X, Deng X, He N, Zheng S (2005) Biosorption and bioreduction of diamine silver complex by *Corynebacterium*. J Chem Technol Biotech 80:285–290